PERGAMON

Available online at www.sciencedirect.com

SCIENCE DIRECT®

Polyhedron 22 (2003) 2013–2017

POLYHEDRON

www.elsevier.com/locate/poly

Density functional study of tetrahedral manganese clusters

Shusuke Yamanaka *, Ryo Takeda, Kizashi Yamaguchi

Department of Chemistry, Graduate School of Science, Osaka University, Toyonaka 560-0043, Japan

Received 6 October 2002; accepted 30 December 2002

Abstract

We have applied the ab initio density functional theory (DFT) based on generalized spin orbital (GSO) for tetrahedral manganese clusters with a noncollinear spin structure. It was found that three-dimensional (3D) spin states become clearly ground-states by all of GSO-localized spin density approximation, GSO-generalized gradient approximation, and GSO-hybrid methods for tetrahedral $Mn(II)_4O_4$. These results are consistent with the experimental results.

Keywords: Generalized spin orbital; Density functional theory; Tetrahedral manganese clusters; Noncollinear molecular magnetism; Hybrid methods; Three-dimensional spin structure

1. Introduction

In the past few decades, multicenter metal clusters have attracted great attentions in relation not only to biomimetic compounds but also to single-molecular magnets (SMMs), both of which the functionality is due to purely the molecular origin [1]. In particular oxo-bridged manganese clusters constitutes an important class among these compounds [2] and are challenging targets of computational chemistry. For instance, the oxo-bridged tetranuclear manganese clusters (Mn_4O_4) are of great interest as the model complex of the photosynthetic water oxidation center [3]. While some researchers investigated the di-μ-oxo manganese dimers from the viewpoints of the magnetic properties [4] and catalyzed reactivities [5], the reports of ab initio calculation of tetranuclear clusters are scanty. However, as for SMM of more high-nulcearity clusters, Zeng et al. conducted discrete variational calculations for Mn_{12}Ac and Fe_{11} at the localized spin density approximation (LSDA) level and suggested the possibility of intramolecular spin-frustration from the intramolecular effective exchange integrals [6]. Pederson and co-workers have computed the magnetic anisotropic energies of Mn_{12}Ac and Mn_{10} [7] clusters using generalized gradient approximation (GGA) solutions for spin–orbit couplings within a perturbational scheme. They showed that the spin-flipped coupling elements contributed significantly to anisotropy barriers in both cases, implying that the spin-canting plays a important role in the intramolecular spin-anisotropy effects although the SMMs have ferrimagnetic structure. Both of these prior results also imply that spin canting is important for the investigation of the ground spin state even though this cluster has an almost ferrimagnetic spin structure. Furthermore, tetranuclear complexes including Mn_4O_2 are reported to be SMMs [8,9]. In particular, Carsto et al. [9] pointed out that intramolecular spin-frustrations play a key role to determine the spin states of a V_4O_2 cluster which was reported to become a SMM. Previously, the present authors pointed out the possibility of the three-dimensional (3D) spin structure for cubane complexes and other high-nuclearity clusters based on classical Heisenberg (HB) model [10]. Thus, the ab initio treatment for noncollinear magnetism is needed.

While the common spin-unrestricted density functional theory (DFT) [11] can be applied for 1D spin density which we call axial spin density wave (ASDW) and of which example is shown in Fig. 1(A), generalized spin orbital (GSO) treatment of DFT is essential for spin-frustrated systems in which competing exchange interactions lead to an energetically preferred 2D spin

---

* Corresponding author. Tel.: +81-6-6850-6111x5566; fax: +81-6-6850-5550.

E-mail address: syama@chem.sci.osaka-u.ac.jp (S. Yamanaka).

0277-5387/03/$ - see front matter © 2003 Elsevier Science Ltd. All rights reserved.
doi:10.1016/S0277-5387(03)00168-2

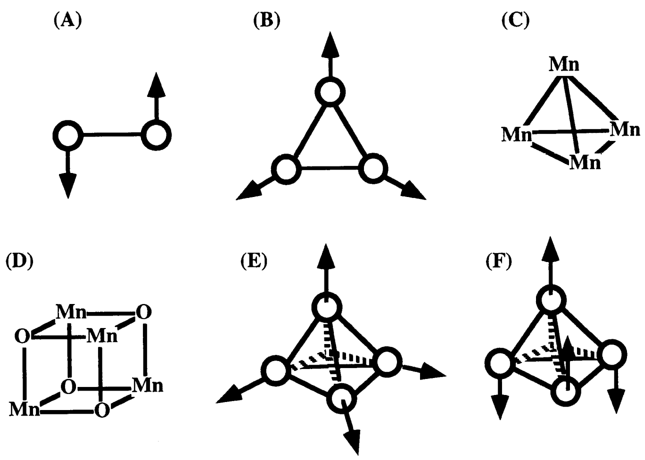

Fig. 1. The collinear (A) and noncollinear (B) spin alignments, the geometries of the tetrahedral manganese cluster (C), Mn_4O_4 (D), and noncollinear (TSW) (E) and collinear (ASDW) (F) spin structures of the tetrahedral manganese cluster.

structure, which was noted as the helical spin density wave (HSDW), as shown in Fig. 1(B). Furthermore, for tetrahedral manganese clusters (Mn_4) illustrated in Fig. 1(C) and the cubane type of Mn_4O_4 shown in Fig. 1(D), 3D spin structure, which we call the torsional spin wave (TSW) state hereafter, illustrated in Fig. 1(E) is conceivable for tetrahedral (T_d) configuration besides ASDW (Fig. 1(F)). By taking GSO-DFT approach presented below, we can describe not only collinear magnetism involving one-dimensional (1D) spin density but also noncollinear magnetism involving two- (2D) or three-dimensional (3D) spin densities. Indeed, we found for hydrogen and chromium clusters that TSWs shown in Fig. 1(E) [12] become ground states by ab initio linear combination gaussian type orbital (LCGTO) GSO-LSDA methods [13]. In this study, we examine ground-states spin structures of GSO-DFT solutions for Mn_4 and Mn_4O_4 having the geometries as in Fig. 1(C) and (D). In addition, we estimate the effective exchange integrals using the HB model scheme [14].

2. Theoretical background

In this section, we briefly present the theoretical background of GSO-DFT approach [13,14] used in our study.

The most essential feature of GSO-DFT is the extension of the constrained search region (CSR) for minimizing the Kohn-Sham (KS) energy functional [4], that is employment of 2 × 2 spin density matrix

$$\rho(\mathbf{r}) = \begin{pmatrix} \rho_{\alpha\alpha}(\mathbf{r}) & \rho_{\alpha\beta}(\mathbf{r}) \\ \rho_{\beta\alpha}(\mathbf{r}) & \rho_{\beta\beta}(\mathbf{r}) \end{pmatrix} \tag{1}$$

for the fundamental parameter, instead of $\rho_\alpha(\mathbf{r})$ and $\rho_\beta(\mathbf{r})$, and minimization of KS energy functional over all non-interacting N-representable spin density matrices such that

$$\begin{aligned} E_{\mathrm{KS}} &= \min_{Tr\rho(\mathbf{r})=N}\left\{T_{\mathrm{S}}[\rho(\mathbf{r})] + \int d\mathbf{r}\, Tr V_{\mathrm{eff}}(\mathbf{r})\rho(\mathbf{r})\right\} \\ &= \min_{\Phi(\mathbf{r})\to N}\langle\Phi|\hat{T}_s + \hat{V}_{\mathrm{eff}}|\Phi\rangle. \end{aligned} \tag{2}$$

Here $T_{\mathrm{S}}[\rho(\mathbf{r})]$ is the kinetic energy functional of an auxiliary non-interacting KS system involving the effective potential, which we denote $V_{\mathrm{eff}}(\mathbf{r})$. By introducing an exchange-correlation (XC) functional $E_{\mathrm{XC}}[\rho(\mathbf{r})]$, we obtain the following for the set of coupled equations for KS orbitals that construct a KS single-determinant wavefunction,

$$\begin{aligned} &\sum_{\sigma_2}\left[\delta_{\sigma_1\sigma_2}\left\{-\frac{\nabla_i^2}{2} + \int d\mathbf{r}'\frac{n(\mathbf{r}')}{|\mathbf{r}-\mathbf{r}'|}\right\} + \frac{\delta E_{\mathrm{XC}}}{\delta\rho_{\sigma_2\sigma_1}}(\mathbf{r}) \right. \\ &\qquad \left. + V_{\mathrm{ext}}^{\sigma_1\sigma_2}(\mathbf{r})\right]\psi_i^{\sigma_2}(\mathbf{r}) \\ &= \varepsilon_i\psi_i^{\sigma_1}(\mathbf{r}), \end{aligned} \tag{3}$$

where σ_i ($i = 1, 2$) is a spin variable (α or β).

In order to exploit CSR consisting of all non-interacting N-representable spin density matrices given by Eq. (1), the XC functional of the GSO-LSDA [13–15] expressed by

$$\begin{aligned} &E_{\mathrm{XC}}^{\mathrm{GSO\text{-}LSDA}}[\rho_+,\ \rho_-] \\ &\quad = \int d\mathbf{r}(\rho_+(\mathbf{r}) + \rho_-(\mathbf{r}))\varepsilon(\rho_+(\mathbf{r}),\ \rho_-(\mathbf{r})), \end{aligned} \tag{4}$$

must be employed for Eq. (3). The localized up (ρ_+) and down (ρ_-) spin densities are expressed by using the number density $n(\mathbf{r})$ and the pauli matrices' vector $\vec{\sigma}$ as

$$\rho_\pm(\mathbf{r}) = n(\mathbf{r}) \pm |Tr\vec{\sigma}\rho(\mathbf{r})|/2. \tag{5}$$

The XC functional depends on the off-diagonal terms of spin density $\rho(\mathbf{r})$, such that the KS equations become coupled equations like Eq. (3). The extensions to GGA or hybrid methods with generalized Hartree-Fock are straightforward.For the collinear magnetic systems, $\rho(\mathbf{r})$ reduces to $\rho_\alpha(\mathbf{r})$ and $\rho_\beta(\mathbf{r})$, and Eq. (3) to two equations for α and β orbitals, respectively, leading to the standard spin-unrestricted DFT.

We employed the familiar exchange-correlation functionals of three classes: (i) HFS exchange [11] plus the Vosko–Wilk–Nusair fifth (VWN5) correlation functional [16], i.e. SVWN5, as a LSDA, (ii) Becke88 [17]+LYP [18] (BLYP) as a gradient corrected approximation, and (iii) B3LYP [19] as a hybrid approximation. MINI basis sets [20] are used for all calculations. The computational results are presented in the next section.

3. Results and discussion

We examine tetranuclear Mn (II) clusters and the cubane type of Mn_4O_4 illustrated in Fig. 1(C) and (D). Aussoleil et al. has pointed out that all effective exchange integral values are equivalent and negative for the $Mn(II)_4$ complex by fitting experimental temperature-dependent magnetic susceptibility [21]. The geometry of the actual cluster, $(C_{12}H_{14}N_3O\text{-}Mn(II))_4 2H_2O$, is slightly distorted to S_4, however, they suggested that the distortion does not induce measurable differences concerning effective exchange integrals, i.e. the spin structure. Thus we assume the T_d geometry with the average of experimental inter-manganese distances, 3.37 Å.

We first calculated the bare $Mn_4(II)$ (T_d). However, the energies of ASDW and TSW are nearly degenerate within the computational precision. As previously explained for the stability of the TSW state of H_4, we must pay attention to that the XC functional of LSDA based methods, given by Eq. (4), itself does not produce the energy difference between TSW and ASDW, and that all spin states including the highest spin are degenerate exactly if itinerant electrons disappear. Thus this result ascribes to the shrank spin-and-electron densities of manganese cations. Indeed, as presented in Fig. 2, the relative stabilities of TSW states in compare to high-spin states drastically increase for $Mn_4(II)O_4$, of which oxygen anions provide the itinerant electrons between manganese sites.

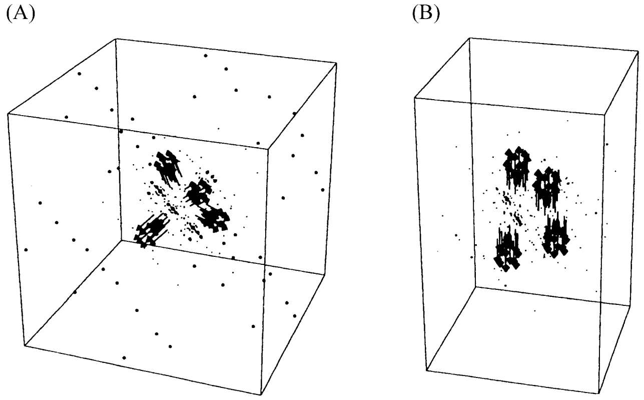

Fig. 3. The Mulliken spin density plots of (A) TSW, and (B) ASDW states of GSO-B3LYP solutions.

Fig. 3 shows the 3D Mulliken spin density plots for the TSW [(A)], and ASDW [(B)] states of $Mn_4(II)O_4$ computed by the GSO-B3LYP. For both states, the spin densities distribute devotedly on the Mn sites, but slightly induced at oxygen sites which are illustrated in Fig. 4 to make the situations clear. It is an interesting point that the spin directions of oxygen sites in TSW states also follows the magnetic ordering of bare manganese sites. The full use of the CSR over 2 × 2 spin density matrices, as in Eq. (2) in the context of DFT, implies that there is no symmetry constraint of the spin-and-time reversal (S × T) group. However, we should note that, if we take the spatial symmetry together with S × T, the spin densities plotted above have double-group tetrahedral symmetries so that they

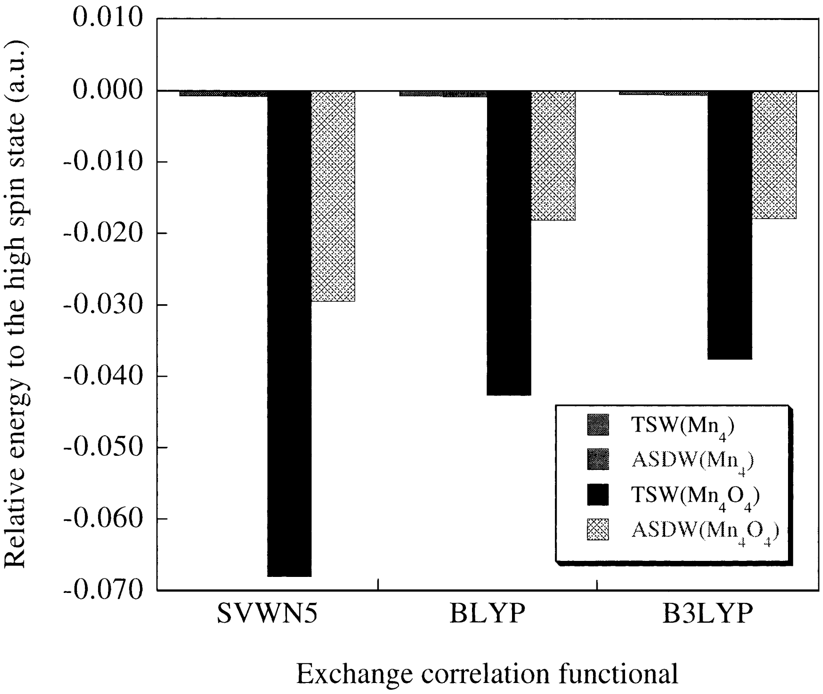

Fig. 2. The relative energies to the high spin state of ASDW and TSW states by GSO-SVWN5, GSO-BLYP, GSO-B3LYP, for Mn_4 and Mn_4O_4.

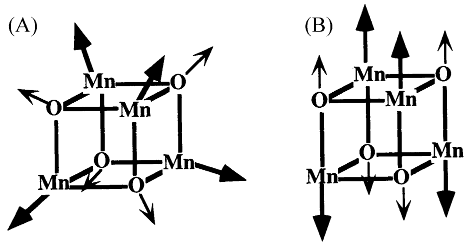

Fig. 4. The schematic illustrations of computed spin structures of (A) TSW, and (B) ASDW states of the Mn_4O_4 cluster.

are admissible as the symmetry-adapted spin alignments for a Hamiltonian involving spin–orbit interactions [22].

Table 1 lists the effective exchange integral (J) values of the HB model calculated by using the TSW and HS computational results as,

$$J = \frac{E_{\rm TSW}^{\rm GSO\text{-}DFT} - E_{\rm HS}^{\rm GSO\text{-}DFT}}{\langle \hat{S}^2 \rangle_{\rm HS} - \langle \hat{S}^2 \rangle_{\rm TSW}}. \quad (6)$$

These magnitudes of the J values for Mn_4O_4 are fairly larger than the experimental value, -0.51 cm^{-1}. The ligand coordination to magnetic sources determine the strength of antiferromagnetic interactions originated from the superexchange mechanism [23], so the computations of these clusters with realistic ligands are needed for quantitative discussions. The J value for bare Mn_4 by GSO-B3LYP is of the same order to experimental value, which might be result by cancelling neglections of both superexchange interactions by anion bridges and these suppression by the electron donations by ligands.

4. Concluding remarks

Ab initio LCGTO GSO-DFT calculations were performed for tetrahedral manganese clusters. We found that the TSW states are most stable for $Mn(II)_4O_4$, which is consistent with the experimentally reported J values. The present result serves to strength the previous suggestion [10,13] that the TSW state is plausible for realistic Mn_4O_4 and Fe_4S_4 clusters with the T_d symmetry. However the magnitudes of J's calculated by GSO-LSDA, GGA, hybrid methods are all much larger than the experimental values, indicating that the totally treatment with the realistic ligand, $C_{12}H_{14}N_3O$ in this case, is needed. Further the double group symmetry of the spin density of TSW states stimulates to image the inclusion of spin–orbit (SO) interactions. Since the SO interactions induce orbital currents, the symmetrical consideration of not only the spin density, but also of the state will be needed [24].

Ab initio GSO-DFT method is expected to be efficient for SMM having the intermediate spins [2,9] which have attracted much attention recently. Indeed, Christou [2] described the illustrations of spin-canting for the butterfly unit, Mn_4O_2 which is not only the building block for a high-nuclearity manganese SMM, but also itself SMM. In addition, nevertheless to say, tetrahedral manganese clusters are important for the native [3a] and biomimetic [3b] oxygen evolutions. Previously, we showed that the cleavage from a triplet oxygen molecule to two triplet oxygen atoms can also be described by GSO-DFT [14]. Multi-central metals and oxygens are ubiquitous in active sites of bio-molecules. Therefore the GSO-DFT approach presented here is essential for the investigation of such metalloenzymes based on ab initio molecular dynamic computations [25].

Table 1
The effective exchange integral (J) values of Mn_4O_4 and Mn_4 clusters by GSO-DFT methods

	SVWN5	BLYP	B3LYP	Experiment
$Mn_4(II)O_4$	−149.3	−93.44	−82.50	−0.51
$Mn_4(II)$	−1.72	−1.63	−0.97	

Acknowledgements

This work has been supported by a Grand-in-Aid for Scientific Research on Priority Areas (Nos. 14204061) and by the Ministry of Education, Science, Sports and Culture, through a Grant-in-Aid for Researchment of Young Scientists (B) (No. 13740330).

References

[1] (a) A. Caneschi, D. Gatteschi, C. Sangregorio, R. Sessoli, L. Sorace, A. Cornia, M.A. Novak, C. Pulsen, W. Wernsdorfer, J. Mag. Mag. Mater. 200 (1999) 182;
(b) D. Gatteschi, R. Sessoli, in: O. Kahn (Ed.), Magnetism: A Supramolecular Function, Kluwer Academic Publishers, Dordrecht, 1996, p. 411.
[2] G. Christou, in: O. Kahn (Ed.), Magnetism: A Supramolecular Function, Kluwer Academic Publishers, Dordrecht, 1996, p. 383.
[3] (a) A. Zounl, H.-T. Witt, Y. Kern, P. Fromme, N. Kraub, P. Orth, Nature 409 (2001) 739;
(b) M. Yagi, M. Kaneko, Chem. Rev. 101 (2001) 21.
[4] T. Soda, Y. Kitagawa, T. Onishi, Y. Takano, Y. Shigeta, H. Nagao, Y. Yoshioka, K. Yamaguchi, Chem. Phys. Lett. 319 (2000) 223.
[5] T.C. Brunold, D.R. Gamelin, E.I. Solomon, J. Am. Chem. Soc. 122 (2000) 8511.
[6] Z. Zeng, Z.Y. Duan, D. Guenzburger, Phys. Rev. B 55 (1999) 12552.
[7] (a) M.R. Pederson, S.N. Khanna, Phys. Rev. B 60 (1999) 9566;
(b) J. Kortus, T. Baruah, N. Bernstein, M.R. Pederson, Phys. Rev. B 66 (2002) 92403.
[8] (a) J. Yoo, E.K. Brechin, A. Yamaguchi, M. Nakano, J.C. Huffman, A.L. Maniero, L.-C. Brunel, K. Awaga, H. Ishimoto, G. Christou, D.N. Hendrickson, Inorg. Chem. 39 (2000) 3615;
(b) E. Carolina, Sanudo, V.A. Grillo, M.J. Knapp, J.C. Bollinger, J.C. Huffman, D.N. Hendrickson, G. Christou, Inorg. Chem. 41 (2002) 2441.

[9] S.L. Carsto, Z. Sun, C.M. Grant, J.C. Bollinger, D.N. Hendrickson, G. Christou, J. Am. Chem. Soc. B 120 (1998) 2365.

[10] K. Yamaguchi, S. Yamanaka, M. Nishino, Y. Takano, Y. Kitagawa, H. Nagao, Y. Yoshioka, Theor. Chem. Acc. 102 (1999) 328.

[11] R.G. Parr, W. Yang, Density-Functional Theory of Atoms and Molecules, Oxford University Press, Oxford, 1989.

[12] K. Yamaguchi, Chem. Phys. Lett. 30 (1975) 288.

[13] S. Yamanaka, D. Yamaki, Y. Shigeta, H. Nagao, Y. Yoshioka, N. Suzuki, K. Yamaguchi, Int. J. Quantum Chem. 80 (2000) 664.

[14] S. Yamanaka, T. Ohsaku, D. Yamaki, K. Yamaguchi, Int. J. Quantum Chem. 91 (2003) 376.

[15] U. von Barth, L. Hedin, J. Phys. C Solid State Phys. 5 (1972) 1629.

[16] S.H. Vosko, L. Wilk, M. Nusair, Can. J. Phys. 58 (1980) 1200.

[17] A. Becke, Phys. Rev. A 38 (1988) 3098.

[18] C. Lee, W. Yang, R.G. Parr, Phys. Rev. B 37 (1988) 785.

[19] A. Becke, J. Chem. Phys. 98 (1993) 5648.

[20] S. Hujinaga, Gaussian Basis Sets for Molecular Calculations, Elsevier, Amsterdam, 1984.

[21] J. Aussoleil, P. Cassoux, P. de Loth, J.-P. Tuchagues, Inorg. Chem. 28 (1989) 3051.

[22] (a) C.J. Bradley, A.P. Cracknell, The Mathematical Theory of Symmetry in Solids, Clarendon Press, Oxford, 1972;
(b) M. Ozaki, H. Fukutome, Prog. Theor. Phys. 60 (1978) 1322;
(c) T. Inui, Y. Tanabe, Y. Onodera, Group Theory and Its Applications in Physics, Springer, Berlin, 1990.

[23] Y. Takano, Y. Kitagawa, T. Onishi, Y. Yoshioka, K. Yamaguchi, N. Koga, H. Iwamura, J. Am. Chem. Soc. 124 (2002) 450.

[24] (a) K. Yamaguchi, T. Fueno, M. Ozaki, N. Ueyama, A. Nakamura, Chem. Phys. Lett. 168 (1990) 56;
(b) M. Ozaki, Prog. Theor. Phys. 62 (1979) 1133.

[25] J. Gao, M.A. Thompson (Ed.), Combined Quantum Mechanical and Molecular Mechanics Methods, ACS, Symposium Series 712, American Chemical Society, Washington, DC, 1998.